Journal of Molecular Liquids 340 (2021) 117219

Contents lists available at ScienceDirect

Journal of Molecular Liquids

journal homepage: www.elsevier.com/locate/molliq

Synthesis and mesomorphic characterization of some novel steroidal mesogens: A structure–property correlation

Vanishree Bhat S [a], V.A. Raghunathan [a], Sandeep Kumar [a,b,*]

[a] Raman Research Institute, Soft Condensed Matter group, C. V. Raman Avenue, Bangalore 560080, India
[b] Department of Chemistry, Nitte Meenakshi Institute of Technology (NMIT), Yelahanka, Bangalore, India

ARTICLE INFO

Article history:
Received 9 June 2021
Revised 4 August 2021
Accepted 8 August 2021
Available online 12 August 2021

Keywords:
Liquid crystals
Ergosterol
Stigmasterol
Cholesterol
Sterol benzoates
Organogelators

ABSTRACT

The steroidal derivatives are found to be extremely good mesogens since their inception. Because of their inherent chirality, they have the potential to induce a wide variety of liquid crystalline phases, including frustrated phases depending upon the structure of the steroidal skeleton and the substituents attached. In this report, a series of novel monoalkoxy and dialkoxy benzoate derivatives of ergosterol and a few monoalkoxy derivatives of stigmasterol have been synthesized and their mesomorphic property has been investigated. The derivatives exhibited various mesophases including SmA, SmC*, N*, TGB and blue phases. Also, the gelation ability of some of these derivatives with various organic solvents has been examined. Furthermore, the mesomorphism of these derivatives has been compared with the analogous cholesteryl counterparts.

1. Introduction:

Liquid crystalline materials, associated with both order and mobility, have gained ample attention due to their self-assembly behavior which can be utilized in various applications. The introduction of chirality in such systems is found to have a profound effect both in molecular as well as in supramolecular echelons [1]. Chiral LCs are fascinating as they are known to exhibit inimitable supramolecular assemblies and rare physical properties. Sterols, one of the important classes of biologically active organic compounds, form a vital source of chiral mesophases due to their unique structural characteristics. Sterols are one of the major components in biological membranes as they have a significant role in the fluidity regulation in the membranes[2,3]. They have been recognized as membrane reinforcers as they influence the mechanical and transport properties of the membranes. The chemical structure of sterols comprises a tetracyclic ring system with the presence of –OH group (at A-ring) and the side chain (usually branched) at the D-ring[4]. This chemical structure infers that the tetracyclic ring contributes to the rigidity and the functionalization of the hydroxyl group with supple tails contributes to the flexibility. This structural contrast manifests in feasibility to organize them in the liquid crystalline form[5,6]. Cholesterol, stigmasterol, β-sitosterol, campesterol, ergosterol are a few examples of sterols with different origins (animals, plants, fungi, etc.), which differ from each other in terms of the number of double bonds and the structure of the side chain. The chemical structures of a few sterols indicating the variation in the steroidal skeleton are shown in Fig. 1.

The structure–property relationship in mesogenic steroidal derivatives is well established in the literature[7,8]. The structural difference in the steroidal skeleton, such as the number and position of the double bond have been reported to influence the liquid crystallinity. The fatty acid esters of stigmasterol, ergosterol, β-sitosterol, etc., have been explored for their mesogenic behavior [9,10] and also the LC property of homologous series of steroidal lipids are well documented[11]. Cholesteryl acetate, studied by Reinitzer was found to exhibit a monotropic cholesteric phase [12], whereas the corresponding acetate of ergosterol was non-mesogenic[10].

The liquid crystalline property of a series of p-n-alkoxy benzoate derivatives of cholesterol was elaborately described by Dave[13] and Vill et al. [14]. They were found to display a variety of mesophases, including cholesteric (N*), smectic A (SmA), smectic C (SmC), and blue phase (BP). Kazuyuki et al. reported a series of mesomorphic cholesteryl 4-n-alkoxy-3-methoxybenzoates[15]. Furthermore, cholesteryl 3,4-dialkoxy benzoate derivatives exhibited enantiotropic cholesteric and smectic A phases, whereas 3,5-dialkoxy and 3,4,5-trialkoxy benzoate derivatives were found to be non-mesomorphic. Also, cholesteryl 4-alkoxy and 3,4-dialkoxy

* Corresponding author.
E-mail address: skumar@rri.res.in (S. Kumar).

https://doi.org/10.1016/j.molliq.2021.117219
0167-7322/

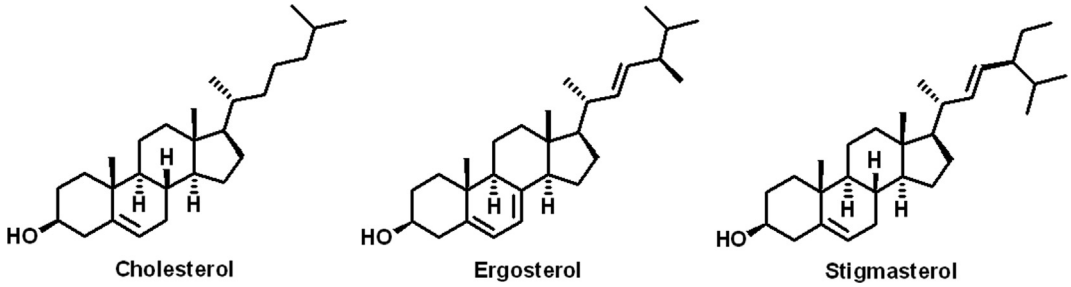

Fig. 1. Chemical structures of cholesterol, ergosterol and stigmasterol.

benzoates were found to show organogelation properties[16], emphasizing the steroidal mesogens as potent organogelators. The effects of chain branching and lateral fluorine substitution on the mesomorphic property of cholesteryl 4-n-alkoxy benzoates have been realized. Mainly, the occurrence of frustrated TGB (twist grain boundary) phase [17–22] in a single benzene ring containing sterol benzoate system was found to be influenced by lateral fluorine substituent and some branched-chain alkanes[23,24]. Literature reports infer that strong molecular chirality (induced by the presence of sterol moiety in steroidal mesogens) results in frustrated phases such as TGB and blue phases[25–27]. Apart from these monomers, there are a substantial amount of cholesterol-based LCs such as dimers[28,29], trimers, tetramers[30], and polymers[31,32] displaying diverse chiral mesophases reported in the literature. But, the studies on mesomorphic properties of the other sterol derivatives are meager compared to the cholesterogens due to their limited availability and comparatively expensive precursors.

In our previous report, the mesomorphic behavior of mercaptoalkyl functionalized sterol derivatives was elaborated[33]. In the present study, a series of alkoxy substituted benzoates of ergosterol and stigmasterol have been synthesized and examined for their mesomorphic properties. The derivatives are found to exhibit diverse mesophases, including N*, SmA, SmC*, TGB_A, and blue phase (BP). The frustrated TGB_A phase that is not commonly observed in cholesterol benzoates was observed in most ergosterol derivatives. A few derivatives were subjected to the gelation studies in various organic solvents and the results are summarized. Furthermore, the variation of mesogenicity with the steroidal skeleton as well as with variable lengths of alkoxy side chains has been discussed and compared with the corresponding cholesteryl derivatives.

2. Results and discussion:

2.1. Synthesis and characterization

The schematic representation of the synthetic route for the ergosterol and the stigmasterol derivatives is shown in Scheme 1 and 2. The synthesis of monoalkoxy derivatives of ergosterol and stigmasterol involves Fisher esterification, Williamson ether synthesis and base-catalyzed ester hydrolysis followed by Stiglich esterification (DCC/DMAP coupling) of the acid with a corresponding sterol (Scheme 1). Whereas, the dialkoxy derivatives were synthesized from 3,4-dihydroxy benzaldehyde (**7**); which is subjected to O-alkylation, followed by the oxidation of the aldehyde to the corresponding acid using $NaClO_2$ and NaH_2PO_4 reagent (Pinnick oxidation), which is then coupled with ergosterol using DCC/DMAP reagent to obtain the target compound **10** (Scheme 2).

The chemical structure and purity of all the synthesized derivatives were analyzed with the help of ^1H NMR, ^{13}C NMR and elemental analysis. Furthermore, the mesomorphic behavior of the purified products is studied with the help of DSC (Differential Scanning Calorimetry), POM (Polarized Optical Microscopy) and XRD (X-ray diffractometry) techniques. The ^1H NMR spectra of these derivatives disclosed the presence of all the peaks present in the corresponding acid as well as the parent sterol devoid of the –COOH and –OH peak, confirming the formation of the ester bond. This is further verified by analyzing the ^{13}C NMR spectrum, which showed a peak around 166 ppm, indicating the presence of the ester carbonyl carbon. The "trans" conformation of double bond present in the side chain of ergosterol and stigmasterol present at position 22–23 of the steroidal skeleton is retained as such in the synthesized derivatives also, which is evident from the value of the coupling constant (*J* in Hz) calculated from the ^1H NMR spectra which is found to be 15 Hz. Further, the data acquired from the elemental analysis is in good agreement with the data which is calculated for the corresponding molecular formula. The detailed synthetic procedure and the spectral data of all the compounds are given in the experimental section of ESI.

Since the sterol moiety induces chirality in these mesogens, the optical rotation studies for the synthesized derivatives have been carried out. From the specific rotation values [α] obtained, all monoalkoxy derivatives of ergosterol as well as the stigmasterol were found to be laevorotatory. The corresponding specific rotation values are listed in **Table S1** (ESI).

2.2. Mesophase characterization:

All the final compounds except the dialkoxy derivative **10f** (Scheme 2) were found to be mesomorphic. The thermotropic mesomorphic behavior of all the synthesized compounds was realized by employing a combination of DSC[34], POM[35], and XRD [36] studies.

2.2.1. Phase transitional behavior and thermal stability of monoalkoxy derivatives (*5a-5j* and *6a-6g*):

The POM and DSC are the preliminary analytical tools to analyze the liquid crystallinity of the synthesized derivatives. The phase behavior was studied by observing the sample sandwiched between a clean glass slide and a coverslip under the crossed polarizers by gradually varying the temperature. The derivatives exhibited brilliant colors at different temperatures in the N* phase, which may be due to the unwinding of the helical pitch, which can be calibrated to a specific temperature[37]. The different textural patterns observed are explained below. Some of the POM textures are shown in Figs. 2, and 4. The polarized optical micrographs for the remaining compounds at different temperatures corresponding to different mesophases are shown in **Fig. S3-S12** (ESI).

The DSC of all the compounds was carried out by varying the temperature of the sample at a rate of 5 °C/min. The DSC thermograms for some of the monoalkoxy derivatives of ergosterol and stigmasterol are presented in Figs. 3, 6 and the same for the

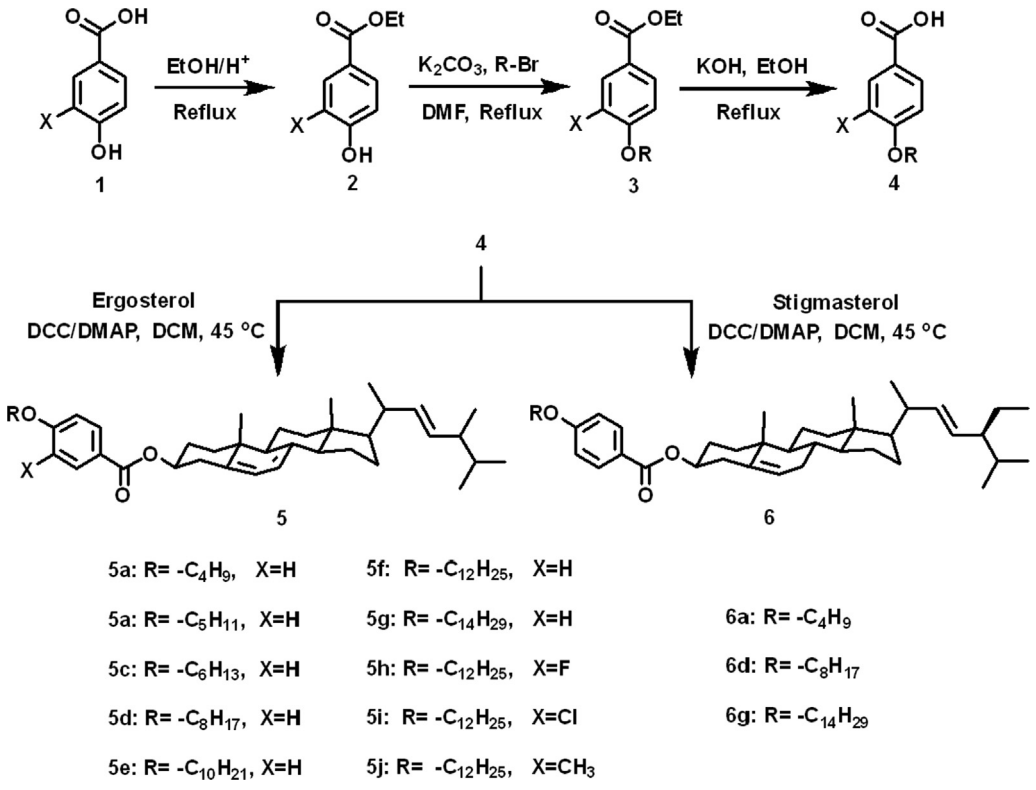

Scheme 1. Synthetic route for ergosterol and stigmasterol 4-(n-alkoxy) benzoates.

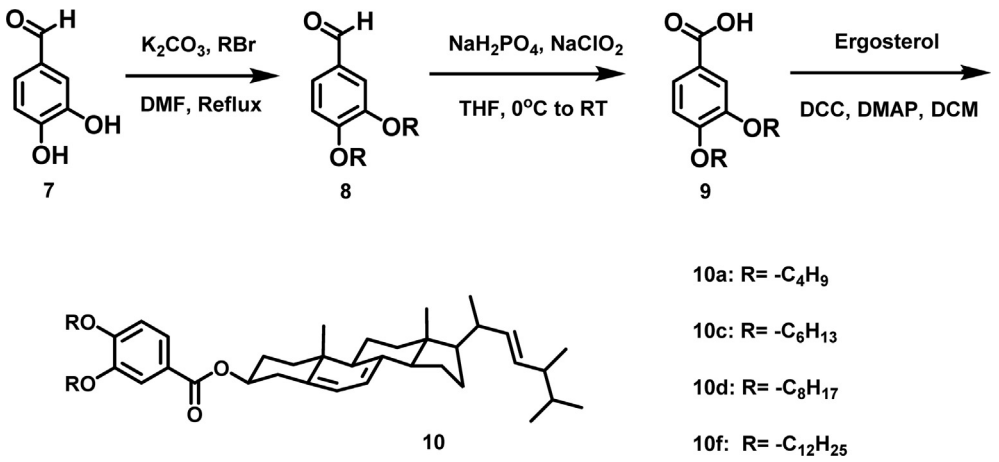

Scheme 2. Synthetic route for ergosterol 3,4 (n-dialkoxy) benzoates.

remaining derivatives is shown in **Fig. S1** (ESI). The mesophase transition temperatures (in °C) with the corresponding enthalpy changes (ΔH in $kJmol^{-1}$) obtained from DSC, both in heating and cooling cycles are summarized and presented in Table 1 and all the synthesized compounds are found to show enantiotropic phase transitions.

The monoalkoxy derivative of ergosterol with C4 chain (**5a**) exhibited two peaks both on heating and cooling (enantiotropic) corresponding to reversible melting (Cr-N*) and clearing (N*-Iso) transitions in DSC (**Fig. 3**). Other derivatives (**5d**-**5g**) displayed a high-temperature cholesteric (N*) phase, which was characterized by the appearance of oily streak texture on heating and focal conic fan texture on cooling, which looks similar to that of SmA mesophase but on mechanical shearing turning into characteristic Grandjean planar texture [38,39] under the crossed polarizers. Since the pitch of the cholesteric phase is highly dependent on the temperature, due to the selective reflection phenomenon, the reflection of different colors in the visible range is observed in cholesteric mesophase as the temperature is lowered[40]. The representative optical micrographs are depicted in Fig. 2**a and 2b**.

The DSC thermograms of **5b, 5c** and **5j** indicated three peaks (Cr-Sm, Sm-N* and N*-Iso) both on heating and cooling (**Fig. 3**), including a peak associated with very low enthalpy change, which can be observed only on magnifying the respective DSC thermogram (**Fig. S2**, ESI) corresponding to reversible Sm-N* phase transition. On heating, when observed optically, **5b** exhibited vibrant

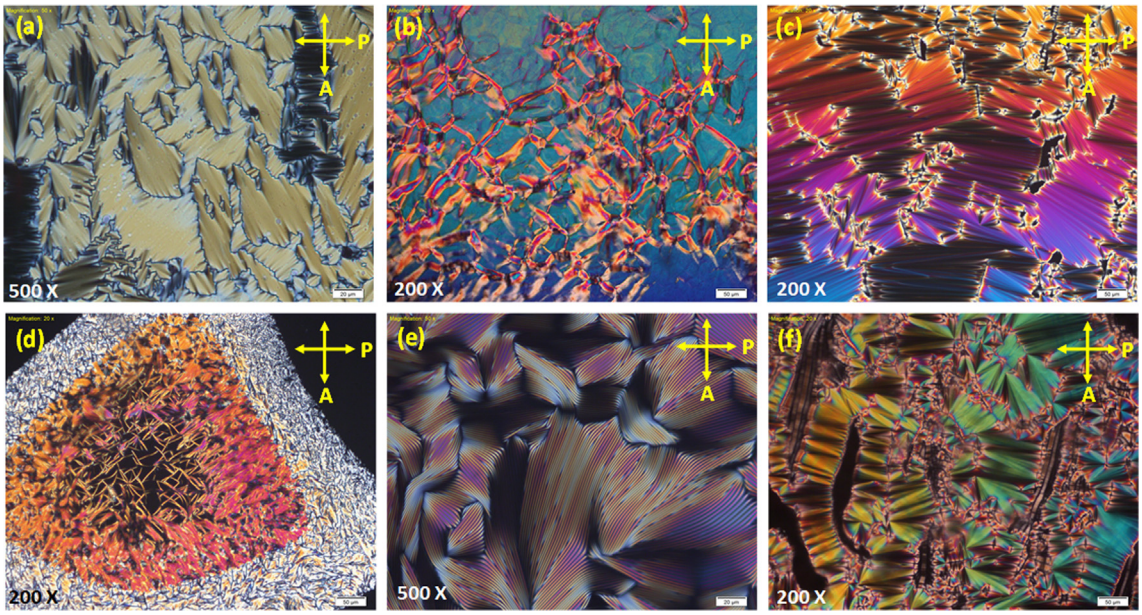

Fig. 2. Optical textures observed in untreated glass slide: (a) Cholesteric or chiral nematic (N*) phase of **5a** on cooling at 175 °C, (b) Oily streak structure of cholesteric phase of **5c** on heating at 181 °C (c) Focal-conic texture of the SmA phase of **5e** on cooling at 143 °C (d) Transition from TGB_A phase to N* phase in **5f** on heating at 174 °C (e) TGB_A phase of **5g** on cooling at 164 °C, (f) Focal-conic texture of the SmA phase of **5h** on cooling at 138 °C.

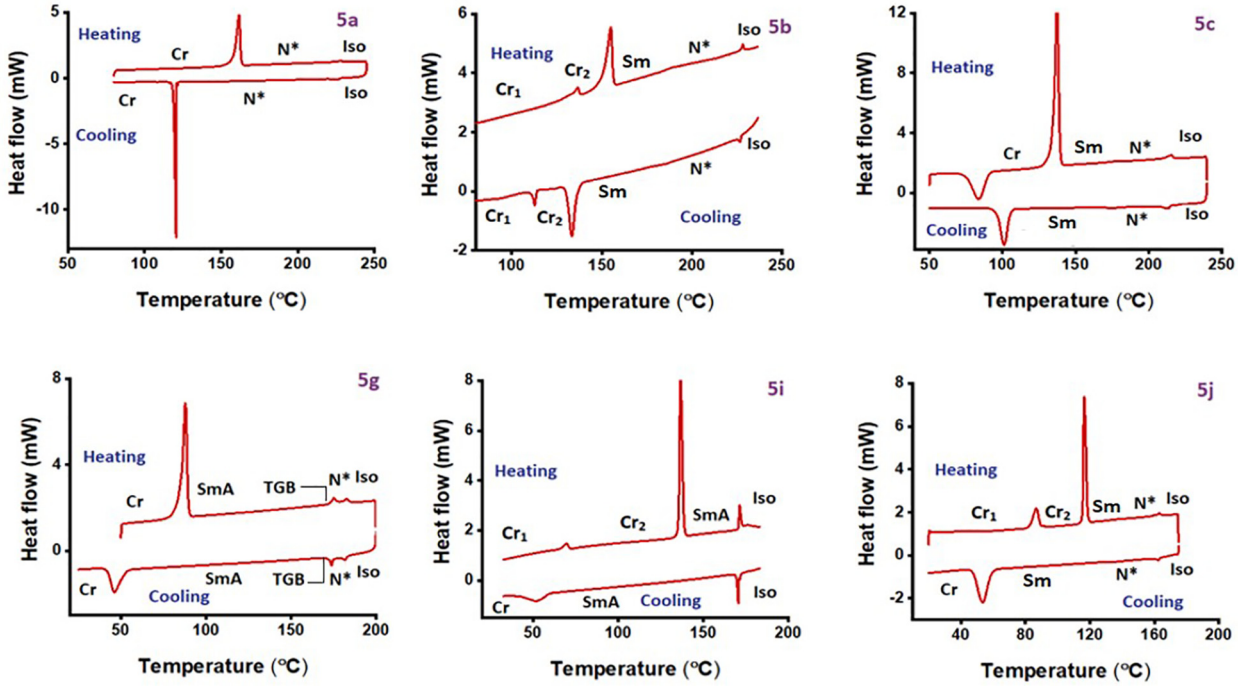

Fig. 3. DSC thermograms of some of the ergosterol derivatives.

colors ranging from red to blue in the visible spectrum between the temperature range of Cr-N* mesophase transition under the microscope (Fig. 4).

On cooling from N* phase, after crossing a specific temperature (180.34 °C in **5b**, 180.92 °C in **5c** and 137 °C in **5j**), the focal conic fan texture of the N* phase turning to oily streak texture [41] on external shearing was more or less retained as such, but a change in the birefringence color along with increased viscosity at lower temperatures was evidenced. The textures observed on heating **5b** is presented in Fig. 4 **(a-c)** and these textural patterns observed were more or less resembling the textures observed for the frozen N* phase by Ooi et al. in cholesterol-containing 'λ' shaped LCs[42].

Since the XRD studies revealed the presence of smectic order in these derivatives, in order to elucidate this phase behavior, derivative **5b** was further investigated using a wedge cell with planar boundary conditions. In these types of cells, since the thickness gradually varies from one edge to another, it results in the formation of an array of equidistant Grandjean-Cano (GC) lines for both N* and TGB phases. On heating, the compound exhibited planar texture with varying colors over which a pattern of fine arcs was

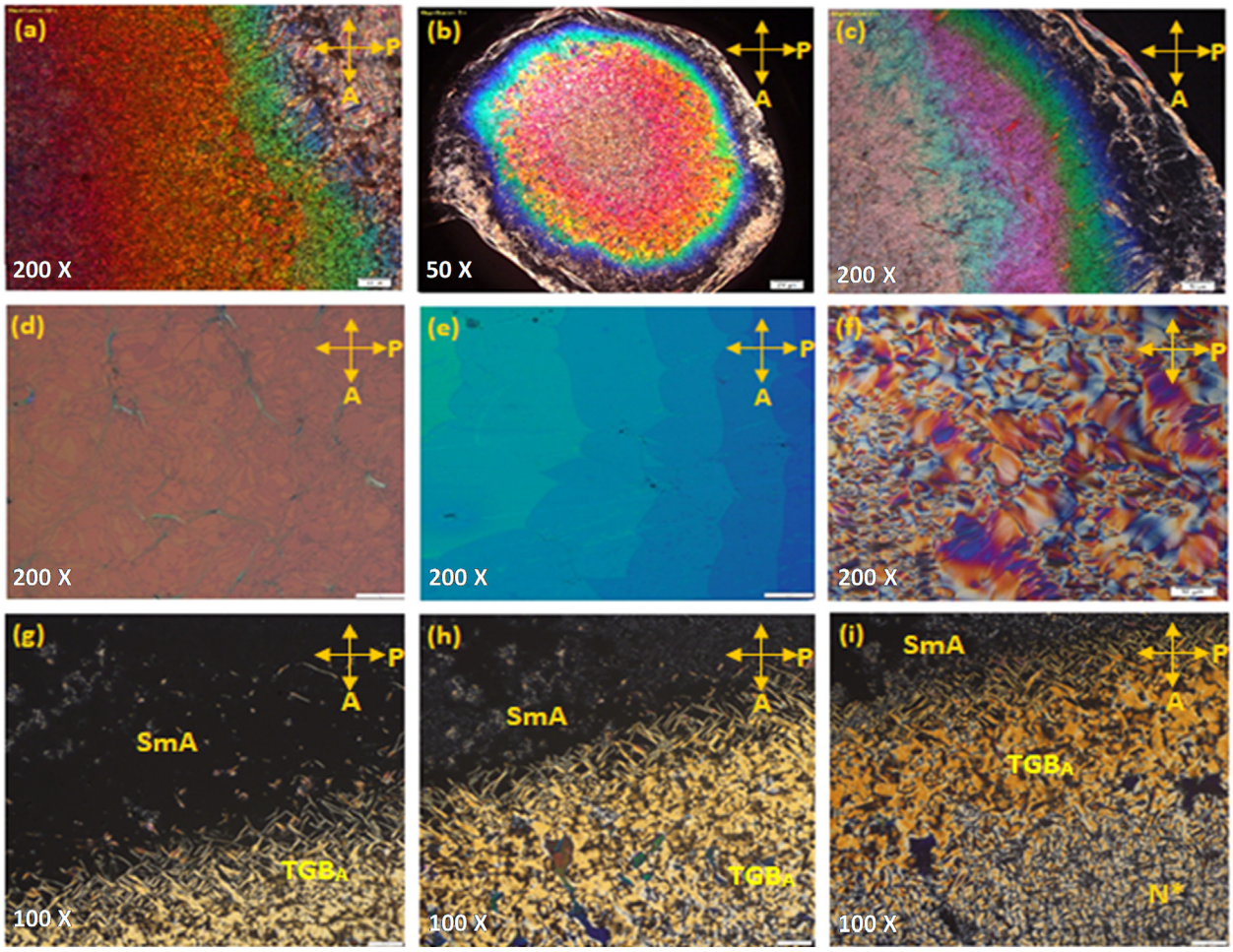

Fig. 4. Polarized optical micrographs of **5b** observed in untreated glass slide on heating at (a) 157.2 °C, (b) 157.8 °C, and (c) at 160 °C. In wedge cell: (d) planar texture on heating at 177 °C, (e) Grandjean-Cano pattern at 175.38 °C on cooling and (f) TGB_A phase observed in **5f** under planar boundary conditions, (g and h) pseudo isotropic SmA phase (dark texture on the top) co-existing with TGB_A phase of **5g** and (i) co-existing SmA, TGB_A and N* mesophases of **5g** under homeotropic boundary conditions.

forming and deforming continuously (from 171 °C). After crossing the Sm-N* transition temperature, the bright color disappeared leaving behind the oily streaks. On cooling from the isotropic melt, GC lines with blue background appeared (at 180 °C), indicating the presence of helical twist in these phases normal to the glass plate (Fig. 4**d, 4e**). Usually, the N* and TGB phases were reported to exhibit these patterns in the wedge cell[43]. Still, the nature of the mesophase appearing below the N* phase is yet to be studied and hence it is represented as SmX mesophase in the present study.

The higher homologs (**5d-5g**) displayed an enantiotropic cholesteric (N*) and smectic mesophases with an intervening TGB_A phase. Cr-Sm phase transition is clearly evident from the DSC thermogram, whereas the phase transition involving Sm-TGB_A is associated with minimal enthalpy change, and hence it is not witnessed in DSC thermograms. Still, the presence of this transient TGB_A phase is evidenced optically, where the growing filamentary textures were observed under the crossed polarizers (Fig. 2**d and 2e**) in an untreated glass slide which resembles the textures observed in the literature[22,44,45]. Furthermore, these derivatives were also studied employing homeotropic (cell coated with ODSE/octadecyl triethoxy silane) and planar (cell coated with polyimide material) boundary conditions[46]. The presence of transient TGB_A phase can be easily identified by the characteristic filamentary texture between homeotropically aligned SmA mesophase (dark region) and the N* phase under homeotropic boundary conditions (Fig. 4**g-4i**) and the typical texture observed for TGB_A phase under planar boundary conditions is shown in Fig. 4**f**. In the derivatives **5f** and **5g**, eventhough not witnessed in DSC**,** on further cooling from SmA mesophase, focal conic texture with equidistant striations was observed under POM, which confirms the presence of SmC* mesophase for a comparatively wide temperature range (around 40 °C). This pattern of equidistant lines is said to be due to the helical superstructures, which are parallel to the smectic layer planes. The distance between two dark lines which are adjacent to each other will determine the pitch of the helix[35].

The effect of -F, -Cl, and $-CH_3$ substituents present ortho to the alkoxy group (with C12 chain) on the LC behavior in the monoalkoxy derivatives of ergosterol has been realized. The presence of lateral fluoro substituent (situated ortho to the ester bond) was found to induce the TGB phase in cholesteryl 2-fluoro 4-n-alkoxybenzoates[23]. In the ergosterol derivatives with the C12 chain, unlike the unsubstituted counterpart, the presence of halogen (-F and -Cl) resulted in the phase sequence involving only the enantiotropic SmA mesophase (**5h** and **5i**). But, no significant decrease in isotropic temperature (4 to 13 °C) was observed. Whereas the phase sequence involving Cr-Sm-N*-Iso transitions was exhibited by ergosteryl 3-methyl 4-n-dodecyloxy benzoate (**5j**) with significantly lower isotropic temperature (163 °C) compared with the unsubstituted counterpart (**5f**).

Furthermore, three stigmasterol derivatives have been synthesized and studied for their mesomorphic behavior (**6a, 6d** and

Table 1
Phase transition temperatures (°C) and the corresponding energy changes (kJ mol^{-1}) given in parenthesis.

Compound	Heating	Cooling
5a	Cr 161.12 (43.99) N* 233.17 (0.77) I	I 227.43 (0.75) N* 122.67 (37.45) Cr
5b	Cr_1 114.86 (11.56) Cr_2 159.66 (31.61) SmX 184.25 (0.26) N* 226.06 (0.88) I	I 224.63 (0.74) N* 180.34 (0.37) SmX 129.69 (22.74) Cr_2 84.58 (3.08) Cr_1
5c	Cr 137.24 (43.58) SmX 181.61 (0.37) N* 215.76 (1.06) I	I 213.57 (1.02) N* 180.92 (0.35) SmX 101.15 (16.09) Cr
5d	Cr 118.72 (17.30) SmA-TGB_A 191.49 (0.85) N* 211.32 (1.16) I	I 209.48 (0.89) N* 188.97 (0.84) TGB_A-SmA 85.53 (13.23) Cr
5e	Cr 117.88 (23.72) SmA-TGB_A 185.57 (1.19) N* 200.74 (1.11) I	I 199.23 (1.12) N* 183.57 (1.24) TGB_A-SmA 72.67 (16.31) Cr
5f	Cr_1 71.99 (4.68) Cr_2 108.46 (17.64) SmA- TGB_A 183.21 (1.34) N* 192.79 (0.79) I	I 190.97 (0.87) N* 181.15 (1.37) TGB_A- SmA 93.00 SmC* 45.49 (2.22) Cr
5g	Cr 87.78 (48.11) SmA-TGB_A 175.01 (1.53) N* 182.68 (0.77) I	I 181.61 (0.72) N* 173.71 (1.53) TGB_A- SmA 91.00 SmC* 46.22 (17.73) Cr
5h	Cr 121.69 (36.06) SmA189.00 (4.90) I	I 188.14 (4.83) SmA 81.19 (21.99) Cr
5i	Cr_1 69.65 (2.02) Cr_2 136.51 (40.13) SmA 171.22 (3.15) I	I 170.48 (4.02) SmA 52.81 (4.04) Cr
5j	Cr_1 86.77 (12.43) Cr_2 116.42 (38.45) SmX 137.91 (0.13) N*162.96 (3.15) I	I 162.43 (0.93) N* 137.10 (0.13) SmX 53.57 (35.33) Cr
6a	Cr 138.29 (31.94) SmA 154.28 (0.49) N* 196.45 (0.41) I	I 191.41 (0.42) BP-N* 152.60 (0.45) SmA 104.60 (27.79) Cr
6d	Cr 96.39 (16.5) SmA 159.02 (1.16) N* 171.52 (0.73) I	I 170.89 (0.71) BP-N* 158.23 (1.14) SmA 80.60 SmC* 46.33 (3.40) Cr
6g	Cr 82.14 (37.91) SmA146.24 (3.59) I	I 143.86 (3.67) SmA 77.7 SmC* 37.64 (19.67) Cr

[Cr = crystal, Sm = smectic phase, N* = chiral nematic/ cholesteric phase, TGB_A =-twist grain boundary A phase, BP = blue phase]

6g). The derivatives **6a** and **6d** exhibited blue phase (BP) for a short temperature range on cooling from the isotropic liquid **(**Fig. 5**a),** which is not evident from the DSC thermogram. Other than this, enantiotropic N* and SmA phases were witnessed in both these derivatives, which are evident from DSC **(**Fig. 6**)** as well as optical observations **(Fig. S10-S11,** ESI**)** with an additional SmC* phase (observed optically) on cooling in **6d (Fig. S11).** On the other hand, **6g** displayed enantiotropic SmA mesophase with characteristic focal conic texture on cooling **(**Fig. 5**b),** which was observed both in DSC and in POM. On further cooling from SmA phase at around 77 °C, focal conic texture with equidistant striations which corresponds to SmC* mesophase **(**Fig. 5**c, Fig. S12)** was observed under the crossed polarizers, which is not evident from the DSC thermogram **(**Fig. 6**).**

2.2.2. X-ray diffraction studies:

To explore the phase behavior of the synthesized compounds, temperature-dependent small-angle and wide-angle X-ray scattering studies (SAXS and WAXS) of the mesogens have been carried out. The derivative **5a** exhibited a broad, diffused small-angle peak and a very broad peak in the wide-angle region around 5.5 Å (commonly observed in all sterol derivatives)[48] confirming the presence of cholesteric (N*) phase **(Fig. S13).** A relatively low-intensity small-angle reflection at low temperatures may be due to the local smectic-like arrangement (cybotactic clusters/Ncyb*) in the cholesteric phase (Fig. 7)[28].

In case of the derivatives **5b**, **5c** and **5j**, on cooling from the isotropic melt, the obtained diffractograms indicated a diffused peak in the small-angle region and a very broad halo in the wide-angle region corresponding to the N* phase as evidenced optically under the crossed polarizers. On further cooling, the sharpness of the small-angle peak gradually increased, signifying the smectic-like arrangement of the molecules. The d-spacing values obtained from the corresponding X-ray diffractograms and the molecular length obtained from Gaussian studies for **5c** and **5j** in all *trans*-form are tabulated in **Table-S2** and **S3** (ESI). The variation of sharpness of the small-angle peak with temperature for **5c** and **5j** is shown in **Fig. S15, S19** (ESI).

The higher homologs of ergosterol (**5d-5g**) and the derivatives of stigmasterol (**6a** and **6d**) reveal a sharp peak in the small-angle region (Fig. 7 and Fig. 11) corresponding to the layer periodicity. In addition, a broad halo is observed in the wide-angle region at around 5.4 Å, which is similar to the wide-angle peaks reported in the literature from liquid crystalline phases of mesogens containing the steroidal skeleton[43,48,49]. Hence we can attribute this peak to the average separation between disordered steroidal cores. Additional diffuse scattering is observed at higher angles in the wide-angle region arising from flexible alkyl chains of the molecules. The comparison of the theoretical molecular length (l) in all *trans*-form acquired from the Gaussian (Fig. 9 **a-c**) and the d-spacing value (d) obtained from the small-angle peak of diffraction patterns indicated the presence of monolayer SmA mesophase since the value of d/l was found to be very close to unity. A similar pattern is observed for all the other derivatives, which exhibited

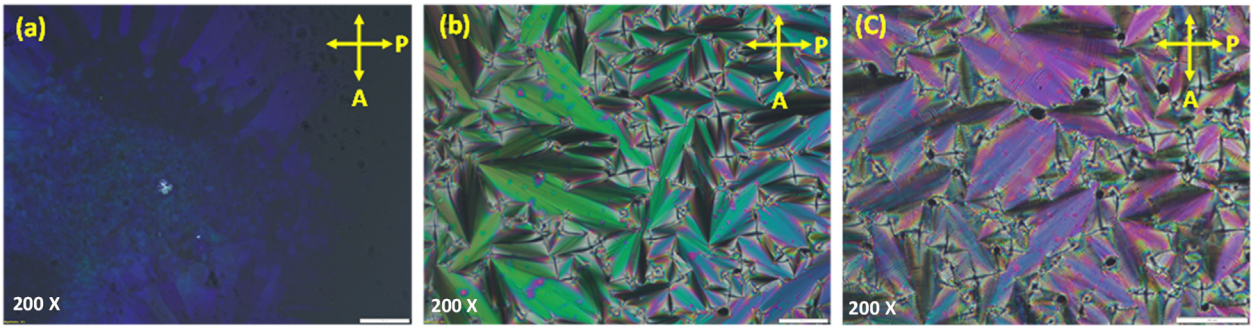

Fig. 5. (a) Platelet texture of blue phase (BP) of **6d** on cooling at 168.2 °C (b) Focal-conic texture of the SmA phase of **6g** on cooling at 109 °C (c) SmC* phase of **6g** on cooling at 77.7 °C[47].

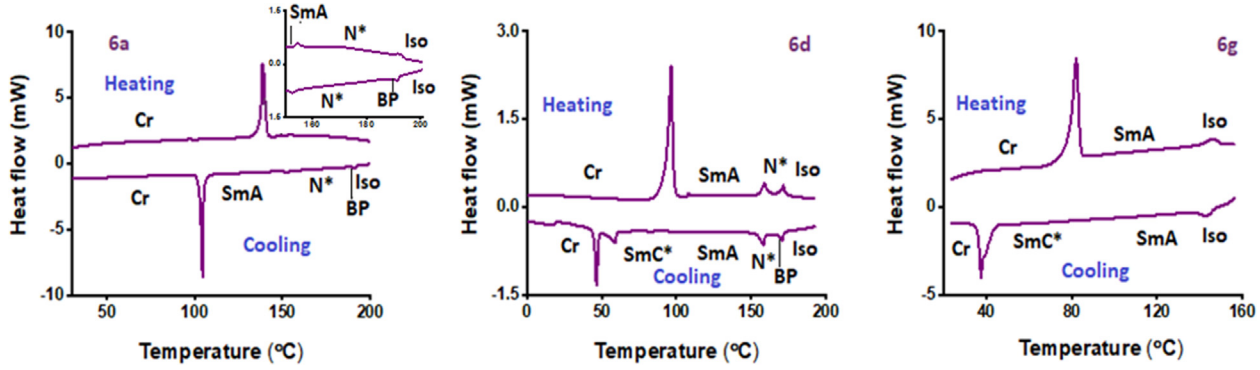

Fig. 6. DSC thermograms for the stigmasterol derivatives.

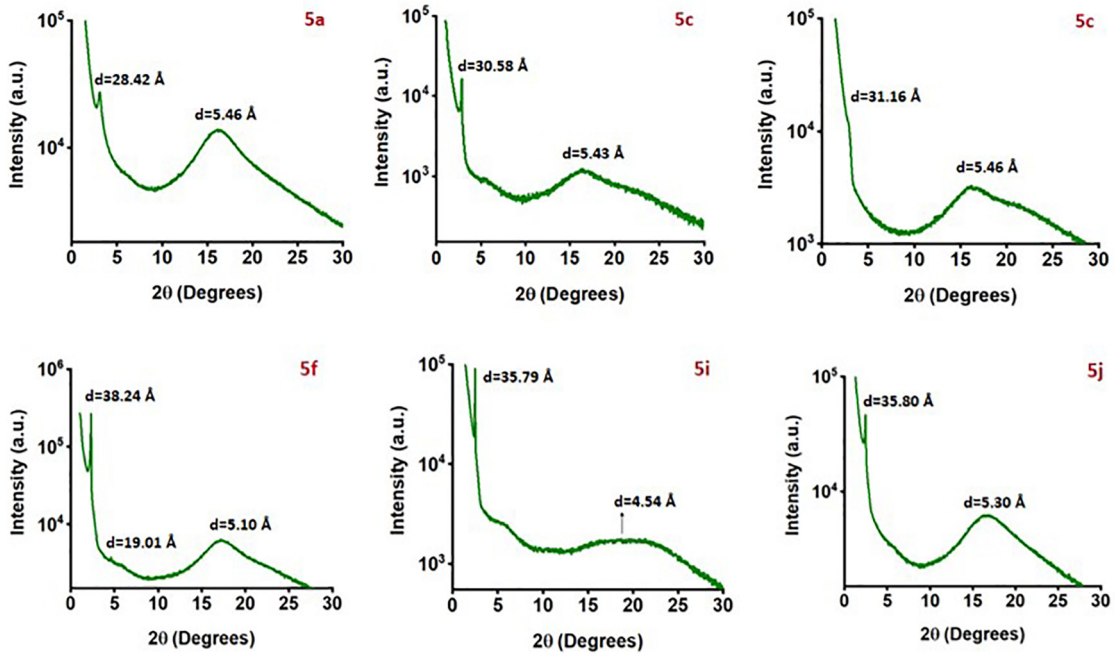

Fig. 7. X-ray diffractograms of **5a** at 170 °C showing cholesteric phase, **5c** displaying smectic and N* phases, **5f** and **5i** showing SmA mesophase and **5j** indicating smectic mesophase.

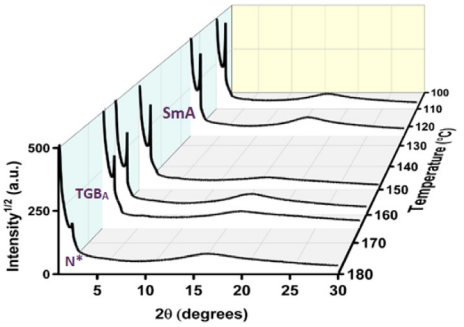

Temperature (°C)	Molecular length (Å)	d-spacing (Å)	d/l
100	38.696	38.38	0.99
140	38.696	37.39	0.97
160	38.696	37.39	0.97
165	38.696	36.98	0.96
175	38.696	36.98	0.96
180	38.696	36.98	0.96

Fig. 8. X-ray diffractogram of **5f** at different temperatures indicating N*-TGB_A-SmA phase transitions and the table indicating the d-spacing values and corresponding d/l value, which is nearly equal to unity.

only the SmA mesophase **(5h, 5i and 6g)**. For some of the derivatives, two peaks with their d-spacing values in the ratio 1:1/2 are witnessed in the small-angle region of XRD, signifying the presence of highly ordered SmA mesophase (Fig. 10). On further heating, the sample from the SmA phase, the sharpness of the small-angle peak decreases gradually and after crossing a certain temperature, a diffused peak in the small-angle region and a broad halo in the wide-angle region were observed, indicating the presence of cholesteric

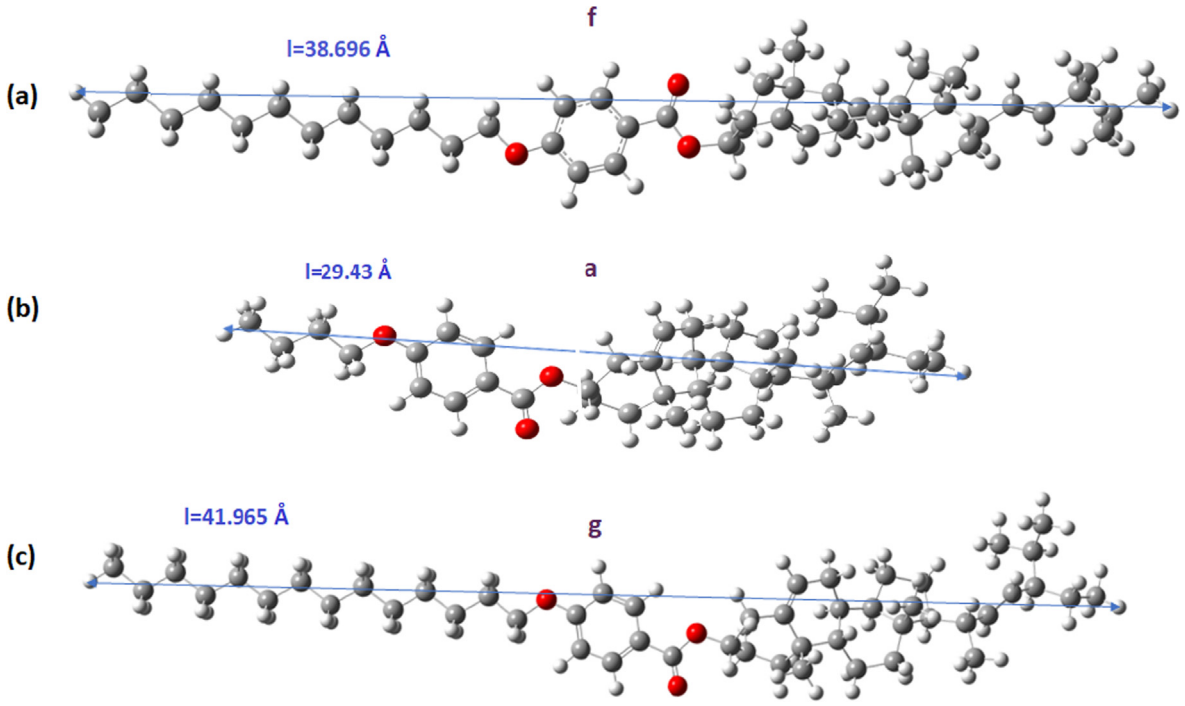

Fig. 9. (a-c): Energy minimized structures for some of the stigmasterol and ergosterol derivatives using b3lyp/6–311 g(d,p) basis set showing rigid-rod like conformation of the derivatives **5f**, **6a**, and **6g**.

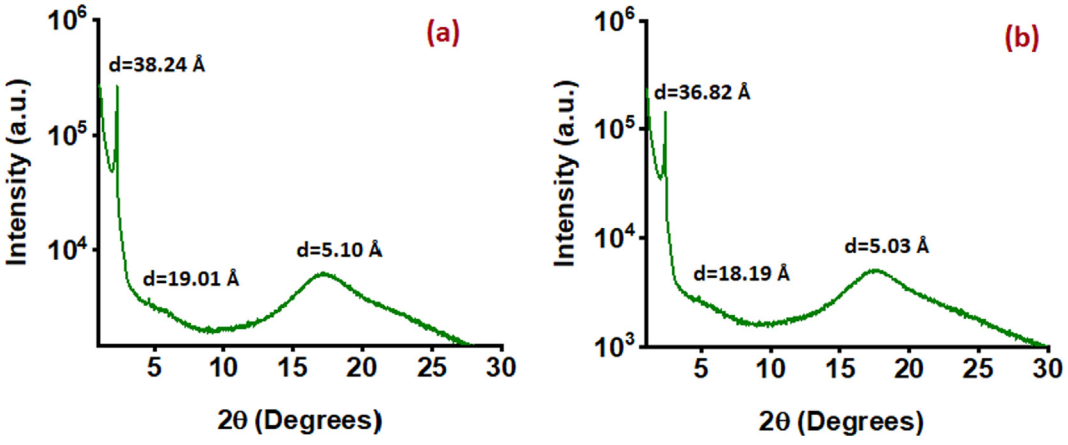

Fig. 10. X-ray diffraction spectra of **5f** on cooling (a) at 110 °C in the SmA regime and (b) at 70 °C in the SmC* regime.

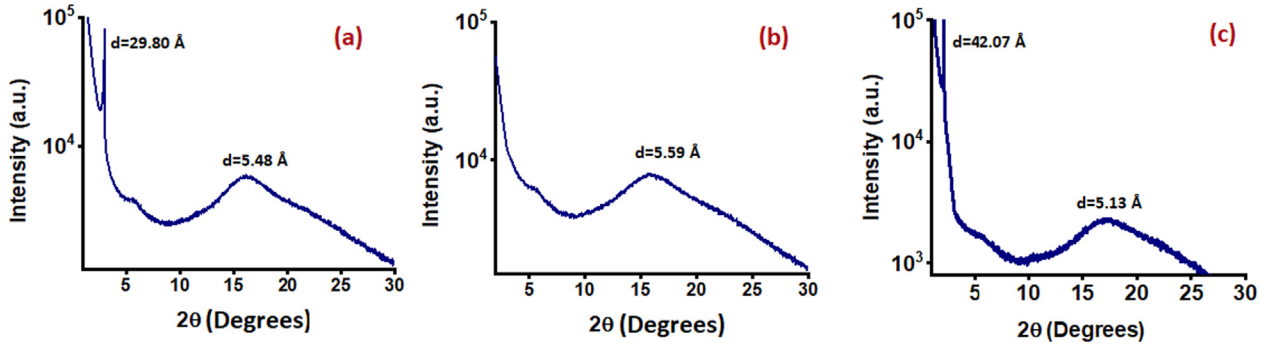

Fig. 11. X-ray diffractograms of (a, b) **6a** on cooling at 150 °C and at 175 °C showing SmA and N* phases respectively and (c) **6g** at 115 °C on heating exhibiting SmA mesophase.

(N*) phase. Variation of the width of the small-angle peak with temperature in the derivatives exhibiting SmA-TGB$_A$-N* phase sequence is graphically represented in Fig. 8 along with the corresponding d-spacing values by considering **5f** as representative. Since the transient TGB$_A$ phase consists of SmA blocks, the XRD pattern obtained for this phase is similar to that of SmA mesophase.

In a few derivatives, the d-spacing value obtained from the intense small-angle peak of diffractogram was found to be smaller than the molecular length of the compound, indicating tilting of the molecules on further cooling from the SmA regime. In such cases, a gradual decrease in the d-spacing value with a decrease in temperature indicates progressive tilting of the molecules[50], and the tilt angle calculated ($\theta = \cos^{-1} d/l$) is found to be around 20–22°. The X-ray diffractograms of **5f** in SmA and SmC* regimes are illustrated in Fig. 10 (**a** and **b**). A schematic representation of the arrangement of the molecules forming the layered structures SmA, SmC*, and TGB$_A$ phase consisting of twisted SmA blocks is illustrated in Fig. 12.

The diffraction patterns observed for some of the ergosterol and stigmasterol derivatives are shown in Fig. 7 and Fig. 11 respectively. The diffractograms obtained for other synthesized derivatives at different temperatures are given in **Fig. S13-S22** (ESI).

Variation of layer spacing (d) with temperature, obtained from the diffraction data, for the ergosterol derivative **5f** and stigmasterol derivative **6g** in the smectic regime is shown in Fig. 13**b**. Both compounds show qualitatively similar behavior. In the SmA phase d increases slightly on decreasing the temperature, and this trend

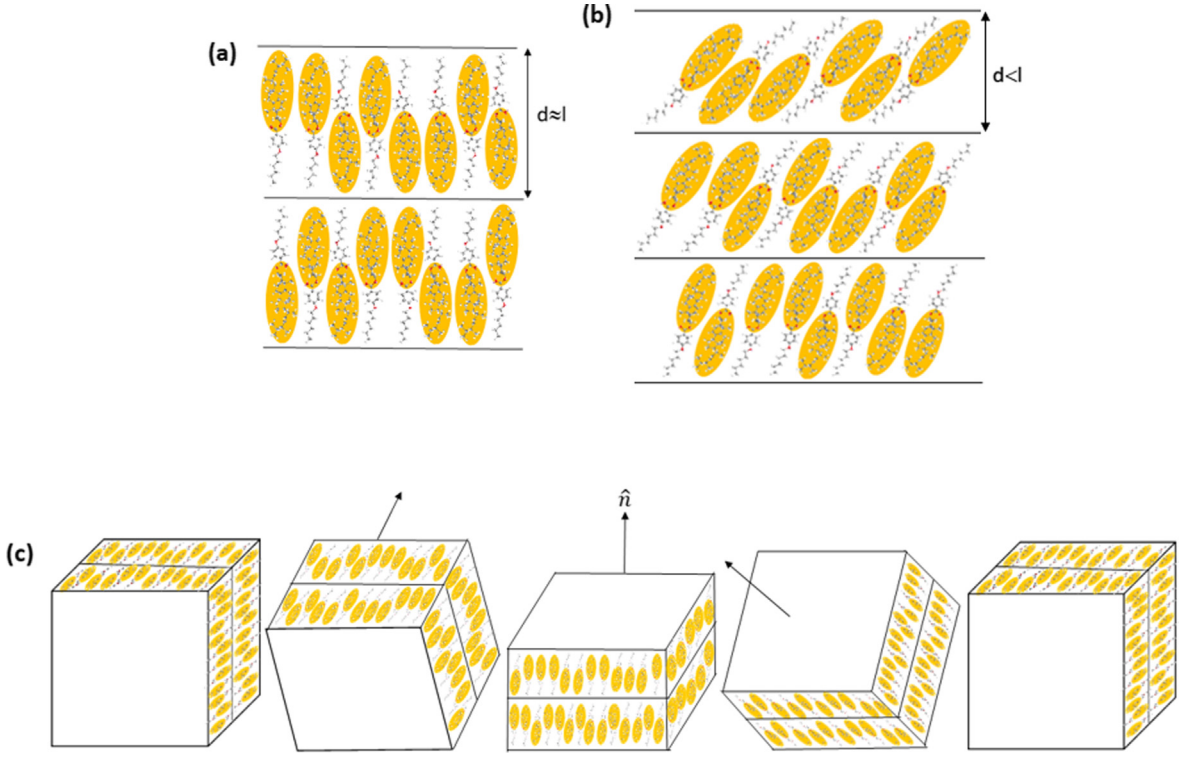

Fig. 12. A schematic representation of the arrangement of molecules in (a) SmA, (b) SmC*[47], and TGB$_A$ phase consisting of SmA blocks [51]

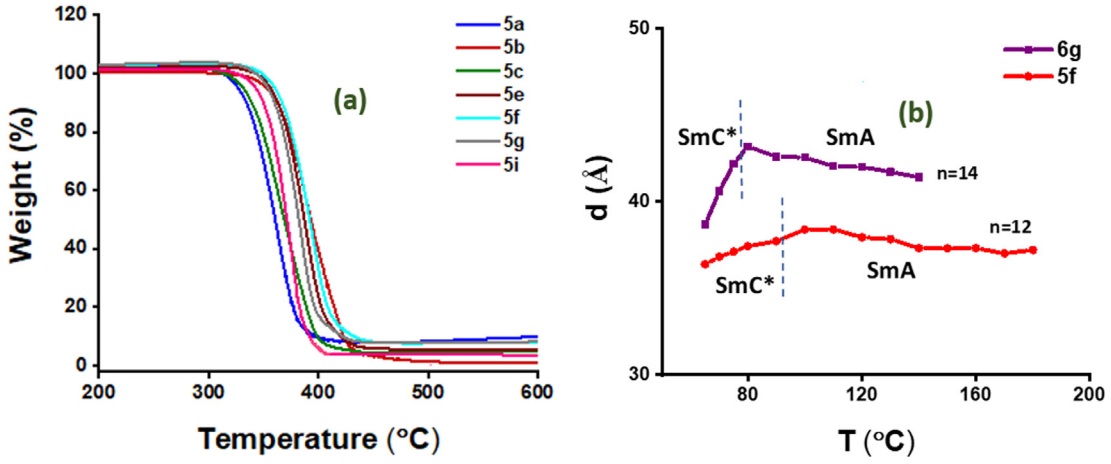

Fig. 13. (a) TGA spectra for the monoalkoxy ergosterol benzoate derivatives and (b) Variation of d-spacing with temperature for the derivatives **5f** and **6g** (on cooling).

is reversed below the SmA-SmC* phase transition. Temperature dependence of d is much more pronounced in the SmC* phase of **6g**. This suggests that the tilt angle in the SmC* phase of **5f** is small and insensitive to the temperature, whereas it increases substantially with decreasing temperature in the SmC* phase of **6g**[52].

2.2.3. Thermal stability of the derivatives:

In order to understand the thermal stability, all the synthesized compounds were subjected to thermogravimetric analysis (TGA). The ergosterol derivatives were found to be stable up to 320 °C and the stigmasterol derivatives upto 300 °C, ruling out the possibility of thermal decomposition of these derivatives while analyzing the mesomorphic behavior (Fig. 13**a**). However, repeated heating and cooling of the ergosterol derivatives is leading to the decomposition because of very high isotropic temperatures.

The variation of isotropic temperature with the alkoxy chain length, with different substituents (-F, -Cl, $-CH_3$) as well as the summary of the phase transition behavior for these derivatives is graphically represented in Fig. 14.

2.3. Gelation studies:

The organogels derived from the compounds with low molecular mass are of great interest as they are promising candidates for numerous biological as well as material applications[53–55]. Generally, organogels are three-dimensional self-assembly of an entangled network of fibrillar structures within which the solvent molecules are entrapped[56]. Low molecular mass organogelators (LMOG), especially those in which the steroidal moiety (S) is tethered to an aromatic core (A) via a supple spacer/linker (L), often called as ALS gelators, are well known in literature[38,57–62] due to their applications in the design of novel functional materials[63].

In previous reports, Kubo et al. had shown the organogelation properties of cholesteryl 4-alkoxy- and 3,4-dialkoxybenzoates in various organic solvents[16]. Similarly, in the present study, a few monoalkoxy derivatives (**6a**, **6g** and **5f**) of stigmasterol and ergosterol benzoates were subjected to gelation studies. The gel samples were prepared by mixing 3.6 wt% of the corresponding sterol derivatives with different solvents (Table 2) in a closed glass vial which is heated to isotropic liquid and kept undisturbed to attain room temperature (RT). The stigmasterol derivatives **6a** readily formed gel in n-decanol on attaining RT, whereas **6g** gelled n-decanol after few hours on attaining RT (Fig. 15).

The morphology of these aggregates was studied using a polarizing optical microscope (POM) and cryo-SEM technique. Under the crossed polarizers, Compound **6a** showed a highly entangled fibrillar network structure, whereas **6g** consisted group of comparatively short fibers. The gel melting temperature (T_{gel}) for **6a** and **6g** were found to be 84 °C and 73 °C, respectively. The fibrillar texture of these organogels as observed under POM is shown in Fig. 16. The gel morphology was further studied by freezing the sample in liquid nitrogen and observing it under the scanning electron microscope (SEM). The Cryo-SEM images indicating the morphology of self-assembled chiral sterol benzoate derivatives are given in Fig. 17.

The X-ray diffraction patterns were recorded for these organogels at different temperatures. These indicate a structure that is partially disordered and partially crystalline. Fig. 18 **(a-c)** show two peaks in the small angle region, whose spacings are in the ratio 1:1/2 which corresponds to a lamellar structure. The broad peak in

Table 2
Gelation test for different compounds.

S. No.	Gel system(3.6 wt%)	Results observed
1.	**6a**-n-decanol	Gel
2.	**6g**-n-hexadecane	Cr
3.	**6g**-dodecane	Cr
4.	**6g**-n-decanol	Gel
5.	**6g**-ethanol	Ins
6.	**6g**-THF	Sol
7.	**5f**-n-hexadecane	Cr
8.	**5f**-dodecane	Cr
9.	**5f**-n-decanol	Cr
10.	**5f**-ethanol	Ins
11.	**5f**-THF	Sol

[Cr = crystallization, Gel = gelation, Sol = solution, Ins = insoluble]

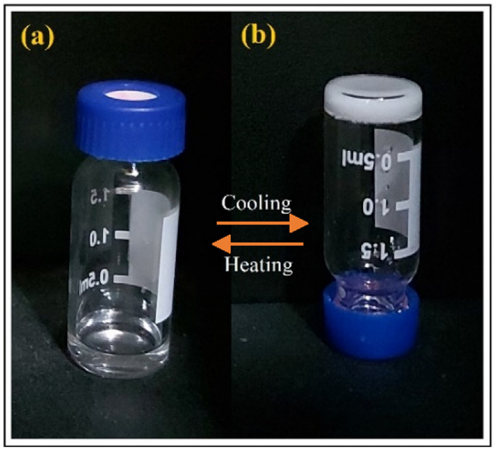

Fig. 15. Photographs of **6g**-n-decanol (3.6 wt%) (a) Isotropic liquid on heating (b) formation of gel on cooling to RT.

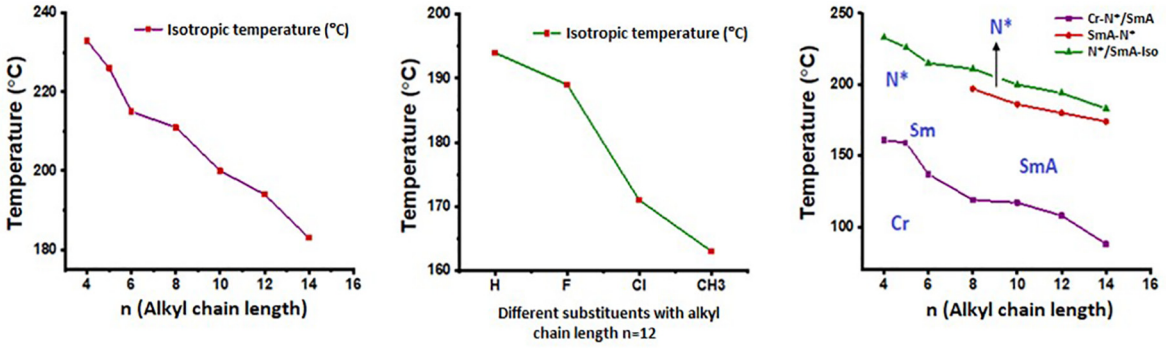

Fig. 14. Summary of the mesomorphic behavior of ergosterol 4-(n-alkoxy) benzoates.

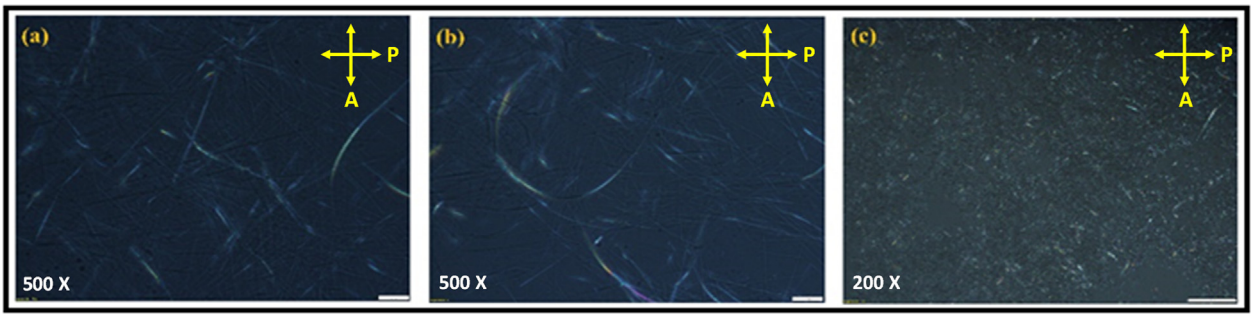

Fig. 16. POM micrographs showing (a and b) fibrillar network of gel formed from the **6a**-n-decanol at RT, (c) fibers of gel of **6g**-n-decanol at RT.

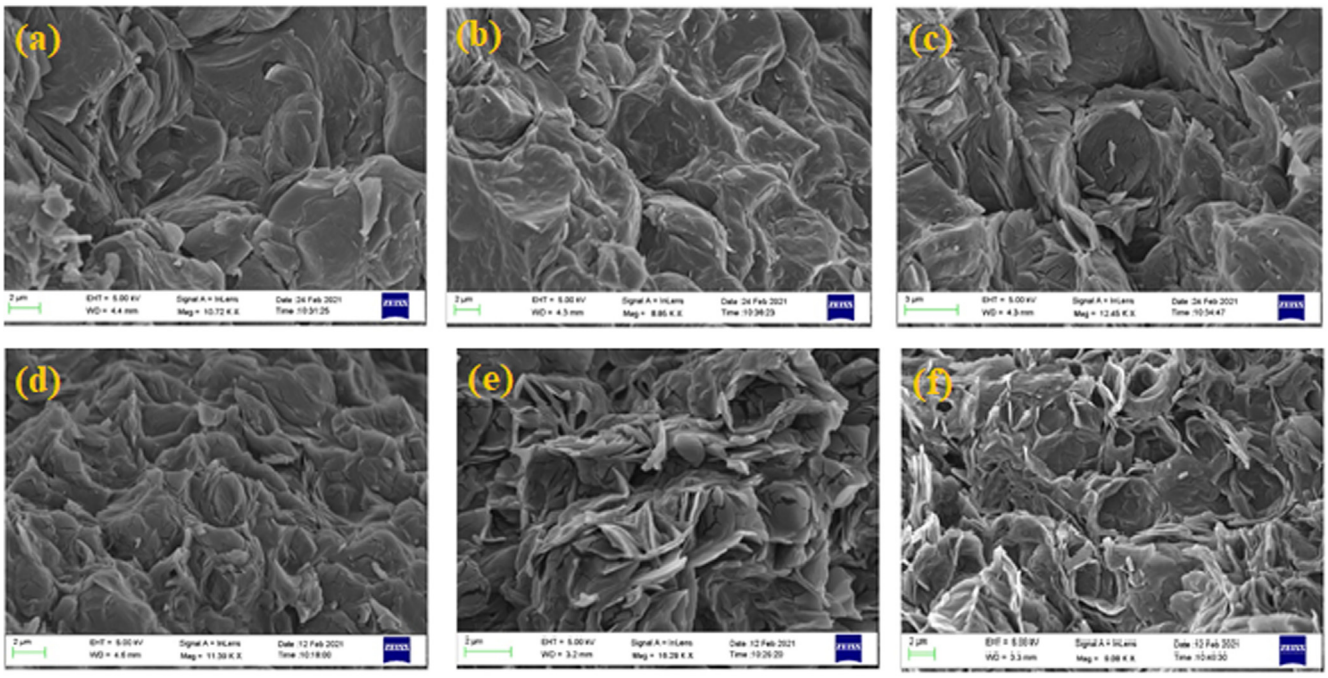

Fig. 17. Cryo-SEM images showing the gel morphology of (a-c) **6a**-n-decanol system within one hour after forming a gel, (d-f) **6g**-n-decanol system (image taken after five days of gel formation).

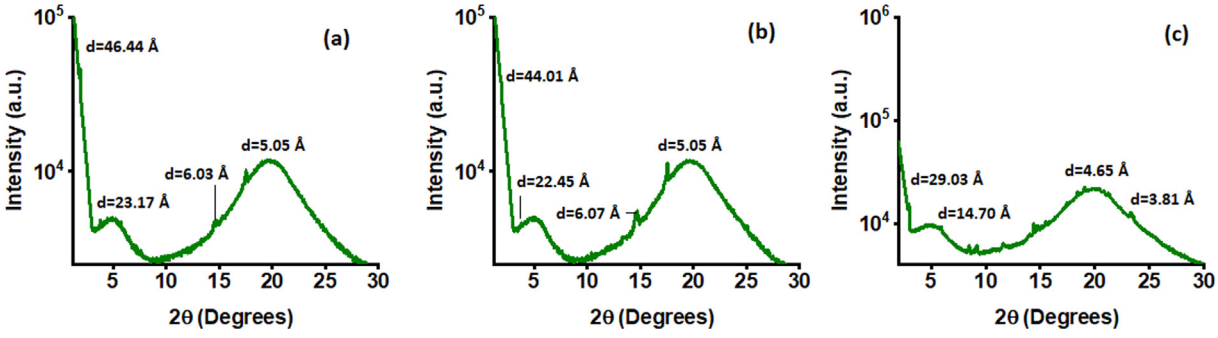

Fig. 18. X-ray diffractograms of (a) **6a**-n-decanol on cooling at 28 °C, (b) **6a**-n-decanol on heating at 30 °C and (c) **6g**-n-decanol on cooling at 28 °C.

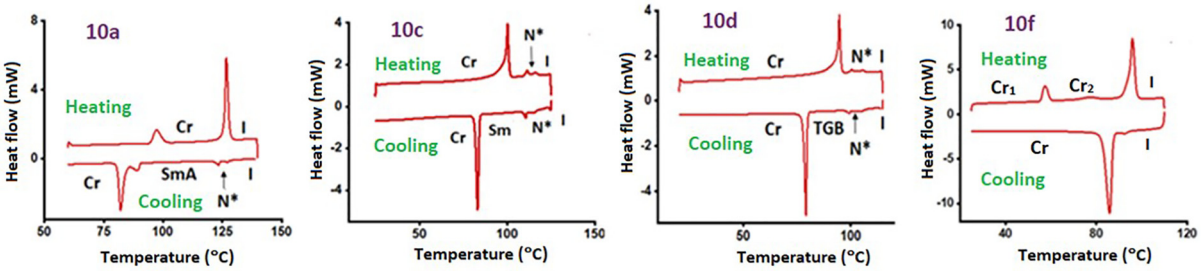

Fig. 19. DSC thermogram for ergosterol (3,4-n-dialkoxy) benzoates **10a**-**10f**.

Table 3
Phase transition temperatures (℃) and the corresponding energy changes (kJ mol^{-1}) for ergosterol (3,4-n-dialkoxy) benzoates.

Compound	Heating	Cooling
10a	Cr_1 97.22 (11.83) Cr_2 127.40 (32.45) I	I 127.35 (0.26) N* 123.44 (1.30) SmA 82.12 (32.31) Cr
10c	Cr 100.15 (22.35) SmA 111.38 (1.18) N* 116.14 (0.5) I	I 115.52 (0.48) N* 110.45 (1.17) SmA 83.09 (24.80) Cr
10d	Cr 94.65 (19.40) TGB_A 100.49 (0.57) N* 105.66 (0.51) I	I 105.11 (0.33) N* 99.29 (0.64) TGB_A 79.11 (24.20) Cr
10f	Cr_1 57.44 (13.83) Cr_2 95.92 (55.97) I	I 85.77 (39.42) Cr

[Cr = crystal; SmA = Smectic-A; N* = chiral nematic/ cholesteric; TGB_A = twist grain boundary A phase.]

the wide angle region indicates a disordered structure, whereas the sharp peaks indicate the presence of crystallites. These patterns arise from the walls separating the cavities (Fig. 17**).**

*2.4. Phase transitional behavior and thermal stability of dialkoxy ergosterol benzoate derivatives (Scheme-2: **10a**-**10f**)*

Similar to the p-n-alkoxy benzoates of ergosterol, (3,4-n-dialkoxy) benzoates exhibited a wide variety of mesophases but for a comparatively short temperature range, whereas the derivative with C12 chain (**10f**) was found to be non-mesomorphic. The DSC thermograms for these derivatives are shown in Fig. 19**,** and the corresponding phase transition temperatures along with the enthalpy changes are tabulated in Table 3. The characteristic focal conic texture of SmA, broken fan texture of N* phase, and thread-like texture of TGB_A phase observed under POM in a thin film of sample sandwiched between an untreated glass slide and coverslip are presented in Fig. 20.

The temperature-dependent X-ray diffraction studies further supported these observations and the X-ray diffractograms of different derivatives at different temperatures are depicted in Fig. 21. The molecular length was obtained from the energy minimized structures (**Fig. S23**, ESI) using Gaussian. The pictorial representation of the arrangement of these dialkoxy derivatives in layered structure forming SmA mesophase is shown in Fig. 23**.**

Further, these derivatives are found to be thermally stable till 250 to 300 °C, as evident from the data obtained from thermogravimetric analysis (Fig. 22). The summary of the phase transition behavior of these dialkoxy derivatives is presented graphically in Fig. 22.

2.5. Comparative analysis of the mesophase behavior:

The mesophase behavior is highly sensitive to the structural changes. In this section, changes in the mesomorphic property of the derivatives with similar functionality and substituted with different steroidal moieties have been discussed and summarized. The p-n alkoxy benzoates of cholesterol were reported to show N* and smectic mesophases with a short range of blue phase on cooling from the isotropic melt[13,14]. Whereas the lower homologs of the ergosterol derivatives exhibited N* phase with a low-temperature mesophase involving smectic order (**5b** and **5c**) and in higher homologs, a sequence involving SmA-N* with a transient TGB_A phase is evidenced, and the temperature range of N* phase is found to decrease with increase in the number of carbon atoms in the alkoxy chain. A low-temperature SmC* phase is witnessed in some of the higher homologs. The isotropic temperature of the lower homologs was less (around 20 °C) compared to the corresponding cholesteryl analogs, whereas no much difference in clearing point was observed for higher homologs. When the sterol moiety is replaced by stigmasterol, a huge fall in the clearing temperature is witnessed (35–40 °C compared to the ergosterol analogs and around 45–50 °C compared with the cholesterol analogs) and the derivatives with C4 and C8 chains (**6a** and **6d**) were involving SmA-N* phase sequence with a short-range BP (blue phase) on cooling. The higher homolog (**6g**) displayed reversible SmA mesophase and a wide range (around 40 °C) SmC* phase, which was also observed in the derivative with C8 chain (**6d**).

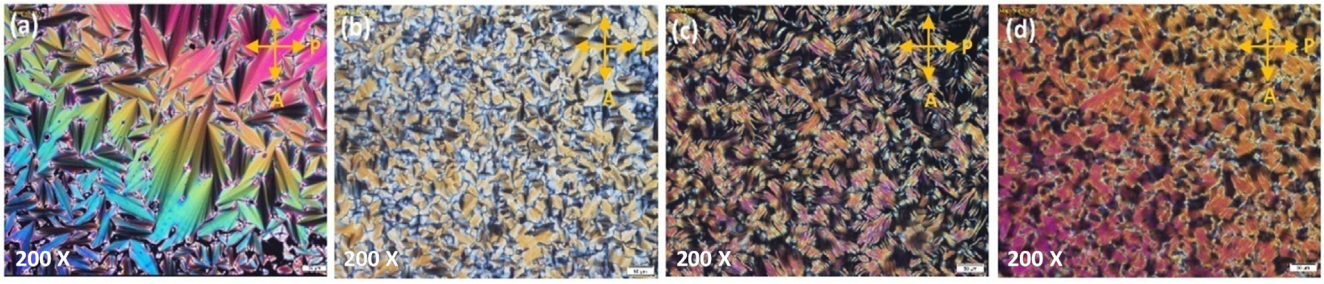

Fig. 20. Optical textures of (a) Smectic A phase of **10a** on cooling at 98.6 °C, (b) Broken fan texture of cholesteric (N*) phase of **10d** on cooling at 97 °C (c & d) TGB_A phase of **10d** on cooling below 96 °C.

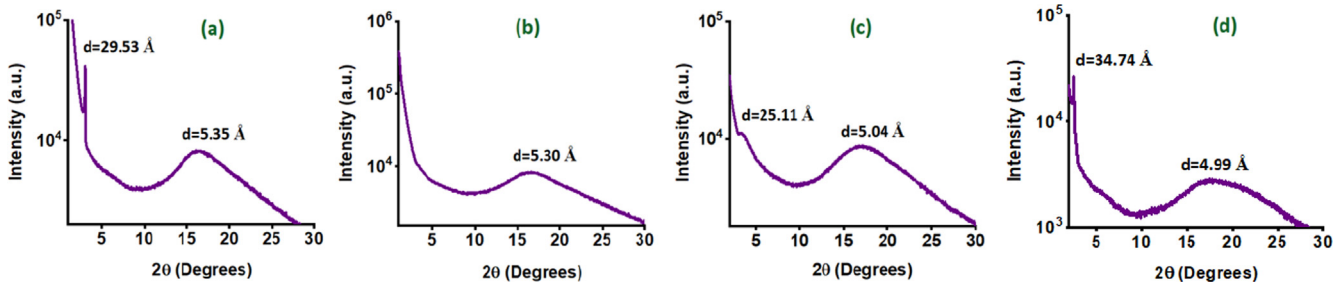

Fig. 21. X-ray diffractograms of (a, b) compound **10a** at 122 °C and at 127 °C indicating SmA and cholesteric (N*) phase respectively, (c) compound **10c** at 112 °C on cooling and (d) compound **10d** at 95 °C on cooling.

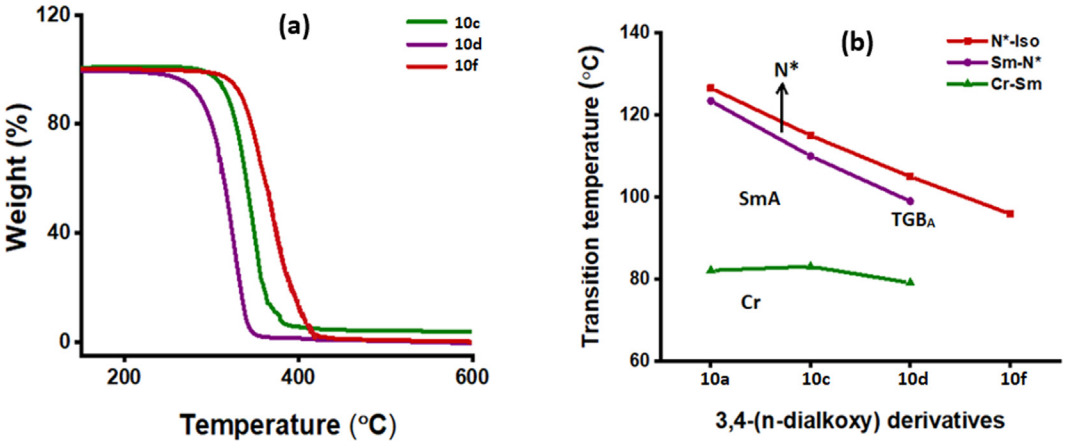

Fig. 22. (a) TGA curves obtained for the dialkoxy ergosterol derivatives indicating the thermal stability of the compounds, and (b) The graphical representation of summary of the phase transition behavior for these derivatives.

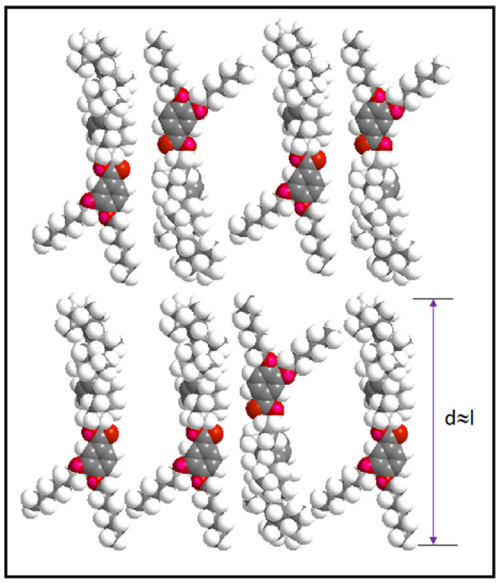

Fig. 23. A model for the arrangement of the molecules of dialkoxy ergosterol derivatives forming layer structure in SmA mesophase.

The 3,4-n-dialkoxy cholesteryl derivatives were reported to show Cr-SmA-N*-Iso phase sequence[16], and the corresponding ergosterol derivatives (**10a-10d**) displayed monotropic and enantiotropic N*, SmA, TGB$_A$ mesophases, and the derivative with C12 chain (**10f**) turned out to be non-mesomorphic. Also, no much variation in the clearing temperature is witnessed for the cholesteryl and ergosteryl derivatives.

3. Conclusion:

In conclusion, a homologous series of monoalkoxy and few dialkoxy derivatives of ergosterol and stigmasterol benzoates have been synthesized and explored for their mesomorphic behavior. The ergosterol derivatives are found to exhibit rich mesomorphic behavior with a wide variety of mesophases such as N*, SmA, TGB$_A$, and SmC*. The effect of substituents such as -F, -Cl, –CH$_3$ present ortho to the alkoxy chain on their LC phase behavior has been discussed. Blue phase (BP), SmA, SmC*, and N* phases were witnessed in the stigmasterol derivatives with considerably less isotropic temperatures (around 35 to 40 °C) compared with the ergosterol analogs. A comparative account of the synthesized derivatives with the cholesteryl counterpart has also been discussed. Further, the gelation property of a few of these derivatives in different organic solvents has been studied.

Declaration of Competing Interest

The authors declare that they have no known competing financial interests or personal relationships that could have appeared to influence the work reported in this paper.

Acknowledgements

The authors thank Mrs. K. N. Vasudha for DSC, XRD, elemental analysis and optical activity studies; Dr. H. T. Srinivasa for NMR and TGA measurements; Mr. K. M. Yatheendran for SEM experiment. Prof. N. V. Madhusudana for valuable suggestions; Dr. Swamynathan K. for the help and guidance. Mr. Marichandran V., Mr. Irla Sivakumar, Ms. Alakananda, Dr. Ashwathanarayana

Gowda, Mr. Subhadip and Dr. Raj Kumar Khan for their useful assistance, co-operation and support. Prof. V. A. Raghunathan thanks the Indian National Science Academy for support through the Senior Scientist Program.

Appendix A. Supplementary data

Supplementary data to this article can be found online at https://doi.org/10.1016/j.molliq.2021.117219.

References

[1] I. Dierking, Chiral Liquid Crystals: Structures, Phases, Effects, Symmetry (Basel). 6 (2014) 444–472, https://doi.org/10.3390/sym6020444.
[2] H. Ohvo-Rekilä, B. Ramstedt, P. Leppimäki, J. Peter Slotte, Cholesterol interactions with phospholipids in membranes, Prog. Lipid Res. (2002), https://doi.org/10.1016/S0163-7827(01)00020-0.
[3] L. Miao, M. Nielsen, J. Thewalt, J.H. Ipsen, M. Bloom, M.J. Zuckermann, O.G. Mouritsen, From lanosterol to cholesterol: Structural evolution and differential effects on lipid bilayers, Biophys. J. (2002), https://doi.org/10.1016/S0006-3495(02)75497-0.
[4] O.D. Sparkman, Z. Penton, F.G. Kitson, 4.5.2 Quadropole ion trap GC-MS, Gas Chromatogr. Mass Spectrom. A Pract. Guid. (2011).
[5] T.P.W. McMullen, R.N.A.H. Lewis, R.N. McElhaney, Cholesterol-phospholipid interactions, the liquid-ordered phase and lipid rafts in model and biological membranes, Curr. Opin. Colloid Interface Sci. (2004), https://doi.org/10.1016/j.cocis.2004.01.007.
[6] C. Paré, M. Lafleur, Polymorphism of POPE/cholesterol system: A 2H nuclear magnetic resonance and infrared spectroscopic investigation, Biophys. J. (1998), https://doi.org/10.1016/S0006-3495(98)74013-5.
[7] G.W. Gray, Advances in Liquid Crystals, 2, Academic press INC. (London) LTD., United Kingdom, 1976.
[8] W. Elser, R.D. Ennulat, Advances in Liquid Crystals, 2, Academic press INC. (London) LTD., United Kingdom, 1976.
[9] J.R. Beveridge, Preparation and Certain Physical Properties 2 (1959).
[10] F.F. Knapp, H.J. Nicholas, Liquid Crystalline Properties of Ergosteryl Fatty Acid Esters, Mol. Cryst. Liq. Cryst. 10 (1970) 173–186, https://doi.org/10.1080/15421407008083493.
[11] T. Thiemann, V. Vill, Homologous series of liquid crystalline steroidal lipids, J. Phys. Chem. Ref. Data. 26 (1997) 291–333, https://doi.org/10.1063/1.556007.
[12] T. Geelhaar, K. Griesar, B. Reckmann, 125 Years of Liquid Crystals–a Scientific Revolution in the Home, Angew. Chem. Int. Ed. Engl. 52 (2013) 8798–8809, https://doi.org/10.1002/anie.201301457.
[13] R.S.V. J.S. Dave, Mesomorphic behaviour of the cholesteryl esters-I: p-n-Alkoxy benzoates of cholesterol, (n.d.).
[14] V. Vill, J. Thiem, Ferroelektrische Cholesterin-Derivate, Zeitschrift Fur Naturforsch. - Sect, J. Phys. Sci. 45 (1990) 1205–1210, https://doi.org/10.1515/zna-1990-9-1021.
[15] K. Kasuga, H. Hatakeyama, Molecular Crystals and Liquid Crystals Synthesis and Thermal . Properties of Cholesteryl 4-n- Alkoxy-3-methoxybenzoates, (n.d.) 37–41.
[16] K. Kubo, K. Tsuji, A. Mori, S. Ujiie, Synthesis and Properties of Cholesteryl Benzoate Derivatives: Liquid Crystals and Organogelators, J. Oleo Sci. 53 (2004) 467–470, https://doi.org/10.5650/jos.53.467.
[17] J.W. Goodby, M.A. Waugh, S.M. Stein, E. Chin, R. Pindak, J.S. Pate, B. Laboratories, M. Hill, T.B. Laboratories, A New Molecular Ordering in Helical Liquid Crystals (1989) 8119–8125.
[18] H.T. Nguyen, C. Destrade, J.P. Parneix, P. Pochat, N. Isaert, C. Girold, T. Cedex, Ferroelectrics TGB A phase in chiral two ring derivatives (2011) 37–41, https://doi.org/10.1080/00150199308217192.
[19] C.V. Yelamaggad, N.L. Bonde, A.S. Achalkumar, D.S. Shankar Rao, S.K. Prasad, A. K. Prajapati, Frustrated liquid crystals: synthesis and mesomorphic behavior of unsymmetrical dimers possessing chiral and fluorescent entities, Chem. Mater. 19 (2007) 2463–2472, https://doi.org/10.1021/cm0625880.
[20] M.B. Pandey, R. Dhar, Electrical properties of frustrated twisted grain boundary phases of liquid crystalline materials, J. Indian Inst. Sci. 89 (2009) 147–167.
[21] D. de Sarkar, R. Deb, N. Chakraborty, G. Mohiuddin, R.K. Nath, V.S.R. Nandiraju, Cholesterol-based dimeric liquid crystals: Synthesis, mesomorphic behaviour of frustrated phases and DFT study, Liq. Cryst. 40 (2013) 468–481, https://doi.org/10.1080/02678292.2012.757814.
[22] T. Seshadri, Novel ferrocene-based chiral Schiff's base derivative with a twist-grain boundary phase (TGBA) and a blue phase, Chem. Commun. (1998) 735–736, https://doi.org/10.1039/a709140k.
[23] S. Shubashree, Twist grain boundary smectic A phase in compounds derived from cholesterol, Curr. Sci. 85 (2003) 1061–1065.
[24] M.C. Varia, H.T. Srinivasa, S. Kumar, Effects of chain branching and lateral fluorine substitution on mesomorphism of cholesteryl benzoates, Liq. Cryst. 41 (2014) 883–890, https://doi.org/10.1080/02678292.2014.882422.
[25] J.W. Goodby, Chirality in liquid crystals, J. Mater. Chem. (1991), https://doi.org/10.1039/jm9910100307.
[26] C.V. Yelamaggad, G. Shanker, Mesomorphic chiral non-symmetrical dimers: Synthesis and characterization, Liq. Cryst. 34 (2007) 799–809, https://doi.org/10.1080/02678290701478921.
[27] R.A. Nayak, S.A. Bhat, G. Shanker, D.S.S. Rao, C.V. Yelamaggad, Highly frustrated liquid crystal phases in optically active dimers: Synthesis and rich phase transitional behavior, New J. Chem. 43 (2019) 2148–2162, https://doi.org/10.1039/c8nj03520b.
[28] C.V. Yelamaggad, G. Shanker, U.S. Hiremath, S.K. Prasad, Cholesterol-based nonsymmetric liquid crystal dimers: An overview, J. Mater. Chem. 18 (2008) 2927–2949, https://doi.org/10.1039/b804579h.
[29] S. Kumar, S.K. Pal, Liquid Crystal Dimers, Cambridge University Press (2017), https://doi.org/10.1017/9781316662120.
[30] A.S. Achalkumar, U.S. Hiremath, D.S.S. Rao, C.V. Yelamaggad, Non-conventional liquid crystals: Synthesis and mesomorphism of non-symmetric trimers and tetramers derived from cholesterol, Liq. Cryst. 38 (2011) 1563–1589, https://doi.org/10.1080/02678292.2011.610473.
[31] V.P. Shibaev, N.A. Platé, Y.S. Freidzon, Thermotropic liquid crystalline polymers. I. Cholesterol-containing polymers and copolymers, J. Polym. Sci. Polym. Chem. Ed. 17 (1979) 1655–1670, https://doi.org/10.1002/pol.1979.170170609.
[32] Y.S. Freidzon, N.I. Boiko, V.P. Shibaev, N.A. Platé, Thermotropic liquid crystalline polymers-22. Optical properties and structure of some cholesteric copolymers, Eur. Polym. J. (1986), https://doi.org/10.1016/0014-3057(86)90207-7.
[33] S. Vanishree Bhat, K. Swamynathan, S. Kumar, Synthesis and mesomorphic characterization of novel liquid crystals derived from bioactive natural sterols, J. Mol. Liq. (2021), https://doi.org/10.1016/j.molliq.2020.115216.
[34] L.M. Blinov, L.M. Blinov, Liquid Crystal Phases (2011) 41–73, https://doi.org/10.1007/978-90-481-8829-1_4.
[35] I. Dierking, Textures of Liquid Crystals, in: Intergovernmental Panel on Climate Change, Clim. Chang. Phys. Sci. Basis (2013) 1–30, https://doi.org/10.1017/CBO9781107415324.004.
[36] L. V Azároff, Molecular Crystals and Liquid Crystals X-Ray Diffraction by Liquid Crystals, (n.d.) 37–41.
[37] A. Taugerbeck, C.J. Booth, Design and Synthesis of Chiral Nematic Liquid Crystals, (2014)
[38] G. Shanker, C.V. Yelamaggad, Synthesis and phase transitional behavior of dimer-like optically active liquid crystals, J. Phys. Chem. B. 115 (2011) 10849–10859, https://doi.org/10.1021/jp206224k.
[39] X. Zhan, X. Jing, C. Wu, Synthesis and mesomorphic properties of a novel series of cholesterol-based liquid crystalline tetramers, Liq. Cryst. 36 (2009) 1349–1354, https://doi.org/10.1080/02678290903229577.
[40] X. Zhan, X. Jing, C. Wu, Synthesis and mesomorphic properties of a novel series of cholesterol-based liquid crystalline tetramers, Liq. Cryst. (2009), https://doi.org/10.1080/02678290903229577.
[41] X. Xu, X. Liu, Q. Li, J. Hu, Q. Chen, L. Yang, Y. Lu, New amphiphilic polycarbonates with side functionalized cholesteryl groups as biomesogenic units: synthesis, structure and liquid crystal behavior, RSC Adv. 7 (2017) 14176–14185, https://doi.org/10.1039/c7ra00360a.
[42] Y.H. Ooi, G.Y. Yeap, λ-Shaped liquid crystal trimers with dual terminal cholesteryl moieties: synthesis and concomitant of N*, SmA and cholesteric glassy phases, Liq. Cryst. 45 (2018) 204–218, https://doi.org/10.1080/02678292.2017.1309701.
[43] A.S. Achalkumar, D.S. Shankar Rao, C.V. Yelamaggad, Non-symmetric dimers comprising chalcone and cholesterol entities: An investigation on structure-property correlations, New J. Chem. 38 (2014) 4235–4248, https://doi.org/10.1039/c4nj00426d.
[44] R. Dhar, Twisted-grain-boundary (TGB) phases: nanostructured liquid-crystal analogue of Abrikosov vortex lattices, Phase Transitions 79 (2006) 175–199, https://doi.org/10.1080/01411590500329819.
[45] R. Dhar, M.B. Pandey, V.K. Agrawal, Twisted Grain Boundary Phases in the Binary Mixtures of 3ß-Chloro-5-Cholestene and 4- N -Decyloxybenzoic Acid, Phase Transitions 76 (2003) 763–780, https://doi.org/10.1080/0141159031000103029.
[46] G. Cordoyiannis, V.S. Rao Jampani, S. Kralj, S. Dhara, V. Tzitzios, G. Basina, G. Nounesis, Z. Kutnjak, C.S. Pati Tripathi, P. Losada-Pérez, D. Jesenek, C. Glorieux, I. Muševič, A. Zidanšek, H. Ameinitsch, J. Thoen, Different modulated structures of topological defects stabilized by adaptive targeting nanoparticles, Soft Matter. (2013), https://doi.org/10.1039/c3sm27644a.
[47] I. Dierking, M. Mitov, M.A. Osipov, Soft Matter Smectic layer instabilities in liquid crystals, Soft Matter. 00 (2014) 1–19, https://doi.org/10.1039/C4SM02505A.
[48] G.Y. Yeap, A. Alshargabi, W.A.K. Mahmood, C.C. Han, H.C. Lin, M. Santo, M.M. Ito, Synthesis, characterization and molecular organization for induced smectic phase of triazole ring in non-symmetric liquid crystalline dimer, Tetrahedron 71 (2015) 3939–3945, https://doi.org/10.1016/j.tet.2015.04.036.
[49] U.S. Hiremath, G.G. Nair, D.S.S. Rao, Supramolecular non-symmetric dimers derived from cholesterol: synthesis and phase transitional properties, Liq. Cryst. 43 (2016) 711–728, https://doi.org/10.1080/02678292.2016.1142010.
[50] G. Shanker, C.V. Yelamaggad, Synthesis and thermal behavior of chiral dimers: Occurrence of highly frustrated and cholesteric liquid crystal phases, New J. Chem. 36 (2012) 918–926, https://doi.org/10.1039/c2nj21035e.
[51] J.W. Goodby, Twist grain boundary and frustrated liquid crystal phases, Curr. Opin. Colloid Interface Sci. 7 (2002) 326–332, https://doi.org/10.1016/S1359-0294(02)00090-0.
[52] G.Y. Yeap, T.N. Chan, W.S. Yam, K. Madrak, D. Pociecha, E. Gorecka, Non-symmetric chiral isoflavone dimers: Synthesis, characterisation and mesomorphic behaviour, Liq. Cryst. 39 (2012) 1041–1047, https://doi.org/10.1080/02678292.2012.693628.

[53] S. Shinkai, K. Murata, Cholesterol-based functional tectons as versatile building-blocks for liquid crystals, organic gels and monolayers, J. Mater. Chem. 8 (1998) 485–495, https://doi.org/10.1039/a704820c.
[54] N.M. Sangeetha, U. Maitra, Supramolecular gels : Functions and uses (2005) 821–836, https://doi.org/10.1039/b417081b.
[55] S. Banerjee, R.K. Das, U. Maitra, Supramolecular gels ' in action ' (2009) 6649–6687, https://doi.org/10.1039/b819218a.
[56] B.Y.P.J. Flory, Introductory Lecture (1974) 7–18.
[57] Y. Lin, B. Kachar, R.G. Weiss, Novel Family of Gelators of Organic Fluids and the Structure of Their Gels ' (1989) 5542–5551.
[58] B.D.J. Abdallah, R.G. Weiss, Organogels and Low Molecular Mass Organic Gelators **, (2000) 1237–1247
[59] P. Terech, R.G. Weiss, Low Molecular Mass Gelators of Organic Liquids and the Properties of Their Gels 2665 (1997).
[60] M. Žini, S. De Luminy, U. De Méditerranée, M. Cedex, Cholesterol-Based Gelators (2005) 39–76.
[61] P.N. One-, T. Organogelators, Pyrene-Derived Novel One- and Two-Component Organogelators (2003), https://doi.org/10.1002/chem.200204459.
[62] A. Chakrabarty, U. Maitra, Organogels from Dimeric Bile Acid Esters : In Situ Formation of Gold Nanoparticles, (2013) 3–10
[63] J.H. Van Esch, B.L. Feringa, New Functional Materials Based on Self-Assembling Organogels : From Serendipity towards Design **, (2000) 2263–2266